MDPI

Article

Responses to Ice Formation and Reasons of Frost Injury in Potato Leaves

Matthias Stegner *, Othmar Buchner, Tanja Schäfernolte, Andreas Holzinger and Gilbert Neuner

Department of Botany, University of Innsbruck, 6020 Innsbruck, Austria
* Correspondence: matthias.stegner@uibk.ac.at

Abstract: Potato leaves are ice-tolerant but are frost-damaged at $-3\,°C$. Freezing occurs in two steps, a first non-destructive freezing event and a second independent lethal event. Localization of ice, and whether cells freeze-dehydrate after the first freezing event remains unknown. The cause of frost damage during the second freezing event lacks experimental evidence. Cytological responses of mesophyll cells were examined during ice formation using cryo-microscopic techniques after high-pressure freeze-fixation and freeze-substitution. CO_2 gas exchange on frozen leaves revealed functional responses, but also frost damage. After the first freezing event, gas exchange was un-interrupted. Consequently, intercellular spaces are free of ice, and ice may be restricted to xylem vessels. The cellular shape of the mesophyll cells was unchanged, cells did not freeze-dehydrate but were supercooled. When thawed after the first freezing event, leaves were initially photoinhibited but regained photosynthesis. During the second freezing event, cells froze intracellularly, and some palisade parenchyma cells remained intact for a prolonged time. Intracellular ice caused complete destruction of cells, and chloroplasts became invisible at the light microscopic level. When thawed after the second freezing, leaves were unable to regain photosynthesis. Consequently, freezing avoidance is the only viable strategy for potatoes to survive frost.

Keywords: freezing-susceptible; freezing stress; frost hardiness; ice nucleation; ice tolerance; *Solanum tuberosum*

1. Introduction

Potato is the fourth most important food crop and is grown in more than 100 countries around the world [1]. Potatoes originate from high elevations in the Andes, an area that lies within the zonobiome of tropical rainforests and the zonobiome of tropical–subtropical monsoon forests and savannahs, and in the lowlands of southern Chile, which lie in the nemoral zonobiome with cold winters and deciduous forests [2]. Optimum growth conditions for potatoes are daily mean temperatures between 18 and 20 °C; further, a frost-free period of approx. 3 months is needed. However, due to climate change, the risk of devastating spring frosts is increasing [3] and will especially negatively affect potato yield in colder regions. Indeed, frost already is a chronic problem for potato production in temperate regions and at high elevations in the tropics [4,5]. At natural field conditions, ice nucleates in leaves of *Solanum tuberosum* between -0.5 and $-3\,°C$ [6,7], and leaves become frost-injured around $-3\,°C$ [8,9]. Potatoes are unable to frost-harden [10,11]. Through infrared differential thermal analysis (IDTA), freezing of potato leaves was shown to proceed in two separate steps [9]. During the first non-destructive freezing event (E1), ice spread extracellularly, first across the xylem but then appearing to capture the entire leaf blade, within 60 s. Potato leaves did not become frost-injured until 10–78 min later, when a second freezing event (E2) occurred, which produced a diffuse freezing pattern without a distinct starting point. This suggests that *S. tuberosum* has ice-tolerant leaves, which were originally only found in other *Solanum* species [8]. However, ice tolerance of leaves of *S. tuberosum* is limited and only possible at moderate temperatures higher

than $-3\ °C$ [12] and short-term frost-exposure [9]. The non-destructive formation of ice must be extracellular. Tolerance of extracellular ice formation is thought to cause cellular freeze-dehydration. Still, the cellular responses of mesophyll cells to E1 at non-destructive temperatures, i.e., whether freeze-dehydration occurs, are unknown.

Potato leaves are lethally damaged by frost during the second freezing process. Without microscopic evidence, this was suggested to be caused by intracellular freezing [9]. Through intracellular freezing ice crystals form within the cell and destroy the protoplasts [13,14]. Intracellular freezing was described to cause the symptom of frost plasmolysis, i.e., loss of osmotic responsiveness, which is observed after thawing of frozen ice in susceptible tissues [14]. However, how intracellular ice formation proceeds is hardly understood, and various symptoms have been observed [14,15]. In these early studies, the measurement technologies employed were limited and without control of freezing and thawing rates; consequently, cellular responses were studied at unnaturally high freezing rates (2–4 $K \cdot min^{-1}$), which might have resulted in supercooling down to between -3 and $-20\ °C$ [14]. As experimental designs can dramatically affect the extent and kind of frost injuries, it must be questioned whether this behavior occurs in nature. How potato mesophyll cells are injured during the second freezing event has not been studied.

We hypothesized that:

(1) After E1, mesophyll cells of potato leaves show freeze-dehydration;
(2) After E1, although it is non-injurious, gas exchange activity stops as ice formation in the intercellular spaces between mesophyll cells blocks gas diffusion;
(3) During E2, the mesophyll cells freeze intracellularly, which causes membrane rupture and irreversibly destroys the cells, resulting in lethality.

During E1, the first non-destructive, and E2, the second lethal freezing event in potato leaves, we aimed to assess functional and cytological responses of mesophyll cells to ice formation. In comparison to unfrozen leaves, we studied the specific cytological responses after E1 through the investigation of frozen, cryo-transferred high-pressure freeze-fixed and freeze-substituted tissue, from which semi-thin sections were prepared and investigated via light microscopy to study the possible occurrence of freezing cytorrhysis. Furthermore, we addressed the physiological performance after E1 and E2 via CO_2 gas exchange measurements. Cellular and structural responses during E2 were studied via cryo-light microscopy.

2. Material and Methods

2.1. Plant Material

Leaves of *Solanum tuberosum* L. (var. Agria Bio) were studied. Plants were grown in the Botanical Gardens of the University in Innsbruck and the University of Salzburg. We used certified tubers, which were grown either in pots (d = 25 cm) embedded in the open field or in natural soil. The soil was sandy silt. The plants were not irrigated artificially and were thus dependent on precipitation at the growing sites. Only fully expanded leaves were sampled. Sampling time was always in the morning. Leaves were cut and kept watered until the start of the experiments.

2.2. Leaf Anatomy

Leaf anatomy was quantified on microscopic sections taken from mature leaves, which were sectioned in off-axis angles of $0°$, $45°$, and $90°$. Five stripes per off-axis angle were sectioned from 3 different leaves. Then, 3 randomly chosen stripes out of the 5 were used to cut 1 section. Sections were cut with a microtome (GSL1, Schenkung Dapples, Zürich, Switzerland) and had a thickness of 80 μm. Analyses were performed using a light microscope (Olympus BX50F, Olympus Corporation, Tokyo, Japan) coupled with a digital camera (Olympus DP25, Olympus Corporation, Tokyo, Japan). Measurements of cells and stomata were performed in the live view mode of the imaging software cell^D 3.1 (Olympus Soft Imaging Solutions GmbH, Muenster, Germany). The leaves of *S. tuberosum* are bifacial (Figure 1) and amphistomatic. At the adaxial leaf side we found 100 ± 12 stomata$\cdot mm^{-2}$;

at the abaxial leaf side, 231 ± 71 stomata·mm^{-2}. The mesophyll palisade parenchyma layer had a thickness of 72 ± 10 µm and the spongy parenchyma layer 116 ± 16 µm. The mean sectional cell area in the spongy parenchyma was 533 ± 252 µm^2 and in the palisade parenchyma 1170 ± 353 µm^2. The area of intercellular spaces was found to be lower than 1%. The leaves had a SLA of 2.32 ± 0.59 (dm^2·g^{-1} DW).
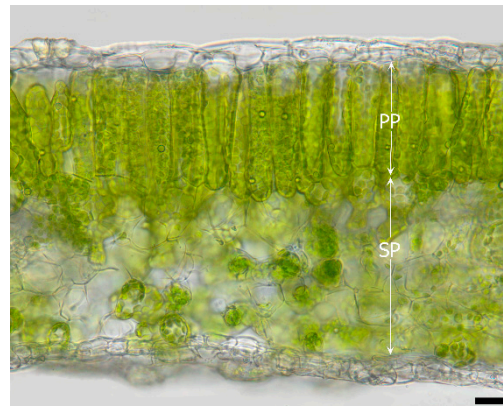
Figure 1. Cross-section of a *Solanum tuberosum* leaf revealing the upper epidermis, the palisade parenchyma (PP) and spongy parenchyma (SP) layers, and the lower epidermis. Off-axis sectioning angle was 90°. Black bar is 20 µm.

2.3. Freezing Treatments

All freezing treatments in the laboratory were conducted in either commercial or laboratory chest freezers. Cooling rates were limited to -3 K·h^{-1}; such rates correspond to naturally occurring leaf-cooling rates at freezing temperatures [6,16].

2.4. Effects of Freezing Events on CO$_2$ Gas Exchange

For gas exchange measurements, leaves from different individuals were used ($n = 3$). The petioles were immediately watered in a test tube, and on the underside of the leaf blade, customized temperature sensors [17] were attached. One sensor recorded the leaf temperature (wire diameter 0.05 mm; COCO-002, Omega Engineering Inc., Stamford, CT, USA), and a second sensor was placed in close proximity (2 mm) to the leaf to measure the reference temperature (TT-TI-40, same manufacturer). The leaves were placed in the standard cuvette of a gas exchange measurement system (GFS 3000, Walz, Effeltrich, Germany), and the entire assembly was transferred into an automatic freezing unit (AFU; ref. [18]). The AFU can be precisely temperature-controlled based on software programmed in LabView 2012 (National Instruments, Austin, TX, USA). After temperature stabilization at +8 °C, the leaves were cooled (-3 K·h^{-1}) to the specific target temperatures. For the detection of leaf-freezing exotherms, the leaf and reference temperatures were recorded at high frequency (1 to 4 Hz). A sudden increase in leaf temperature compared to the reference temperature (DTA, differential thermal analysis [19,20]) allowed detection of leaf ice formation. The leaves were illuminated at 1000 µmol photons·m^{-2}·s^{-1} at temperatures above +4 °C and kept in darkness during cooling below +4 °C.

The effects of freezing processes on CO$_2$ gas exchange and on the viability of the leaves were investigated. Freezing of potato leaves proceeds in two separate steps, a first non-destructive freezing event (E1) and a second event (E2) which is lethal to the leaves [9]. We used two different experimental approaches: (1) After E1, the leaves were kept for several minutes in this state and were quickly thawed and irradiated again, before the occurrence of E2. (2) After E1, the leaves were cooled until E2 was registered. Only after completion of E2 the leaves were thawed and irradiated again.

Before and during the freezing treatment, and after thawing, the assimilation rate (A) and dark respiration rate (R$_D$), respectively, were recorded. Before and immediately after

the experiment, the maximum quantum efficiency of photosystem II was determined through assessment of the chlorophyll fluorescence parameter F_v/F_m.

2.5. Cryo-Microscopy

2.5.1. Semi-Thin Sections of High-Pressure Frozen Leaves

The effect of short-term, non-destructive freezing (E1) on the shape of the mesophyll cells was investigated on semi-thin sections of high-pressure frozen and freeze-substituted leaf samples. For preparation of freeze-fixed samples, leaves from 3 different individuals were detached and frozen (-3 K·h^{-1}) to -2.5 °C. Once ice nucleated, circular areas were punched out from these leaves and immediately fixed in the frozen state by means of high-pressure freeze-fixation (HPF; Leica Empact, Leica Microsystems, Wetzlar, Germany). Controlled freezing was carried out in an Automatic Freezing Unit (AFU; see [18]). The leaves were placed on a polystyrene block and wrapped in cling film to thermally insulate the leaves. Fine wire thermocouple sensors (Type T, solder junction diameter < 0.2 mm, TT-TI-40, Omega Engineering Inc., Stamford, CT, USA) were inserted between the abaxial leaf side and the polystyrene block to monitor the leaf temperatures and to detect the occurrence of freezing exotherms (Figure S1). The petioles were placed in Eppendorf tubes stuffed with cotton wool and filled up with water mixed with a solution of ice-nucleating active (INA) bacteria (*Pseudomonas syringae*; ref. [19]). The INA bacteria triggered ice nucleation at approx. -2.5 °C [21,22]. To ensure that all leaves froze at the same time, based on the method of Kuprian et al. [23], short glass-fiber-coated wires (GG-TI-28, Omega Engineering Inc., Stamford, CT, USA) were soaked in the INA solution, inserted into PVC tubes (to prevent the glass-fiber coating from drying), and then placed in two adjacent Eppendorf tubes. By doing this, once ice nucleated in one leaf, ice quickly spread to the other leaves, so that the leaves froze simultaneously. The whole arrangement was placed in the precooled AFU. After leaf temperatures had stabilized between +4 °C and 0 °C, the temperature was lowered until freezing of the leaves occurred at -2.5 °C. After an exposure time of 20 min at this temperature, leaf discs were collected for the high-pressure fixation (Leica EMPACT, Leica Microsystems, Wetzlar, Germany). Punching out leaf discs and placing them in gold-plated specimen holders (interior dimensions: 1200×200 µm, 16706897, Leica Microsystems, Vienna, Austria) was carried out in the AFU using thermally insulated gloves. Transfer of the prepared specimens to the pre-cooled HPF-device was performed without thawing, so that it was possible to fix the leaf tissue in the frozen state at approx. 12,000 K·s^{-1} and 2040 bar (for details, see [18]). The subsequent freeze-substitution and embedding in epoxy resin was carried out in accordance with a previously published protocol in a Leica EM AFS (Leica Microsystems, Wetzlar, Germany) [24]. Freeze-substitution was performed at -80 °C in acetone containing 2% OsO_4 and 0.05% uranyl acetate. The samples were epoxy-resin-embedded and heat-polymerized.

Semi-thin sections (0.6 µm) were prepared at a Reichert Ultracut S (Leica Microsystems, Wetzlar, Germany). The sections were transferred onto glass slides and stained with 0.3% Toluidine Blue O [25] and investigated with a Zeiss Axiovert 200 M microscope, and images were captured with a Zeiss AxioCam HRc camera (Carl Zeiss, Jena, Germany).

2.5.2. Cross-Sections Viewed by Light Microscope

To address cellular responses during leaf freezing, leaf cross-sections ($n = 3$) were monitored and captured using a Leica DM1000 light microscope (Leica Microsystems, Wetzlar, Germany) while being exposed to sub-zero temperatures. The freezing treatments were conducted inside a temperature-controlled chest freezer (GT 21012, Liebherr, Lienz, Austria), equipped with fans, to avoid temperature gradients, as described in detail by Kuprian et al. [26]. The microscope was equipped with a camera (Leica EC4, Leica Microsystems, Wetzlar, Germany), and the whole unit was placed inside the freezer. The software LAS EZ 3.0.0 (Leica Microsystems GmbH, Wetzlar, Germany) was used for live view and image capture. An acrylic glass lid with integrated thermally insulated gloves on top of the freezer enabled operation of the microscope throughout the freezing treatment.

Cross-sections were prepared with a microtome (GSL1, Schenkung Dapples, Zürich, Switzerland) in an off-axis cutting angle of 90° and a section thickness of 80 μm. To guarantee hydration and facilitate ice nucleation, a small ball of moist cotton wool inoculated with INA bacteria was placed on the microscope slide at the margin of the coverslip. From the cotton wool, a thin thread was elongated underneath the coverslip alongside the cross-section. A thermocouple was installed next to the cotton wool to detect freezing. Target temperature was −2.5 °C.

3. Results

A typical freezing response of a *S. tuberosum* leaf, with two temporally separated freezing events, shows E1, which was followed by E2 (Figure 2). E1 was registered at −1.0 °C and E2 at −2.5 °C. E2 was detected 48 min after E1. While E1 is a short-time event releasing little heat, E2 lasts for several minutes and produces a significant amount of heat.
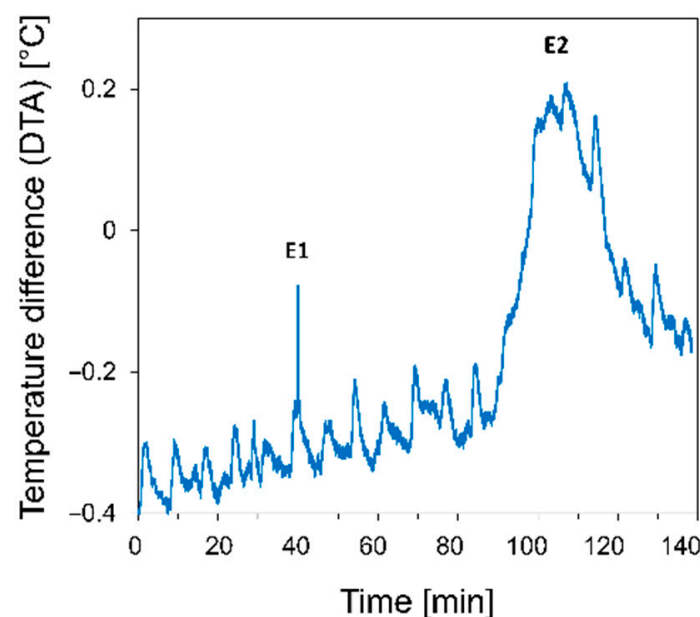
Figure 2. Characteristic freezing response of a leaf of *Solanum tuberosum* during a controlled freezing treatment down to −4 °C. Two temporally separated freezing exotherms occurred; the first freezing event (E1) was registered at −1.0 °C, and 48 min later, the second freezing event (E2) at −2.5 °C.

3.1. Responses to the First Freezing Event

3.1.1. Cytological Aspects

Leaves of *S. tuberosum* were immediately freeze-fixed after E1. The shape of epidermal, palisade, and spongy parenchyma cells of unfrozen control cells (Figure 3A) had the same appearance as the respective cells after the freezing event, which appeared unaffected by E1, i.e. the cells did not freeze-dehydrate (Figure 3B,C).

3.1.2. Gas Exchange and Photosystem II

CO_2 gas exchange of *S. tuberosum* leaves was continuously recorded during controlled freezing treatments (Figure 4). Before the treatment, leaves had a Photosystem II efficiency (F_v/F_m) > 0.8. In the example shown, the assimilation rate (A) was about +1.6 μmol CO_2 $m^{-2} \cdot s^{-1}$. During low-temperature exposure, leaves were darkened, and a constant dark respiration rate (R_d) of approximately −0.5 μmol CO_2 $m^{-2} \cdot s^{-1}$ was recorded. When the first freezing exotherm (E1) was registered at −1.2 °C, the leaves were kept at this temperature for 24 min. Strikingly, R_D was unaffected by E1. Thereafter, the leaf was rapidly thawed, and irradiation was switched on again. After thawing, the assimilation rate rapidly reached its initial value. F_v/F_m remained temporarily reduced to 0.35 but recovered to 0.74 within the next day. After E1, the leaves were always fully intact and did

not show any symptoms of frost injury. Similar gas exchange responses were found on *S. tuberosum* leaves during and after exposure to −7 °C that had been kept free of ice in an unfrozen state for a prolonged time period (data not shown).
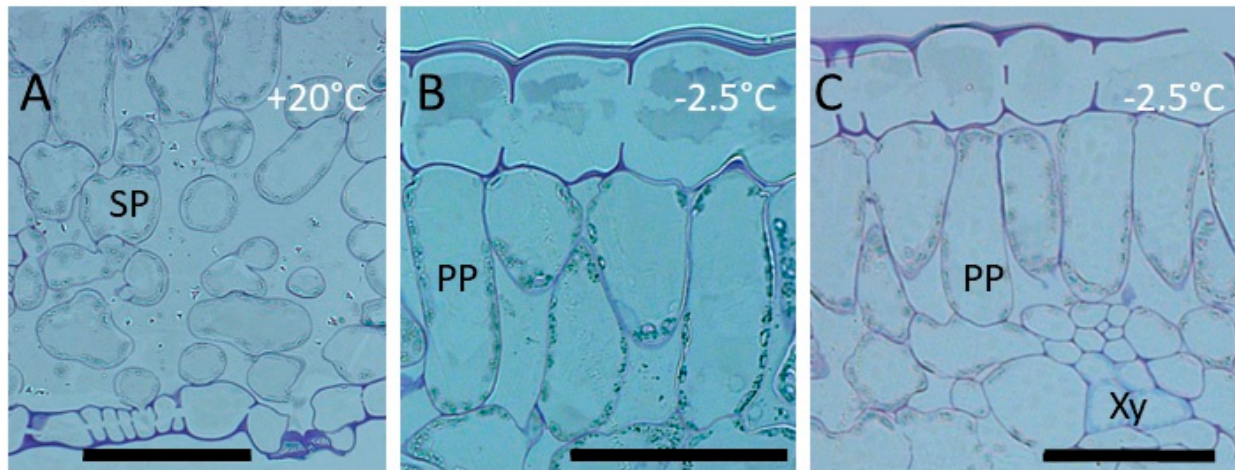
Figure 3. Semi-thin sections (0.6 μm) of high-pressure frozen, freeze-substituted, and epoxy-resin-embedded leaves of *Solanum tuberosum*. (**A**) Untreated controls fixed at 20 °C: lower epidermis, spongy parenchyma (SP) cells, and lower end of palisade parenchyma (PP) cells. (**B,C**) Frozen leaves fixed after the first freezing event (E1) at −2.5 °C: upper epidermis, palisade parenchyma cells, and in C, spongy parenchyma cells and xylem (Xy) tissue of a vascular bundle. Scale bars 50 μm.
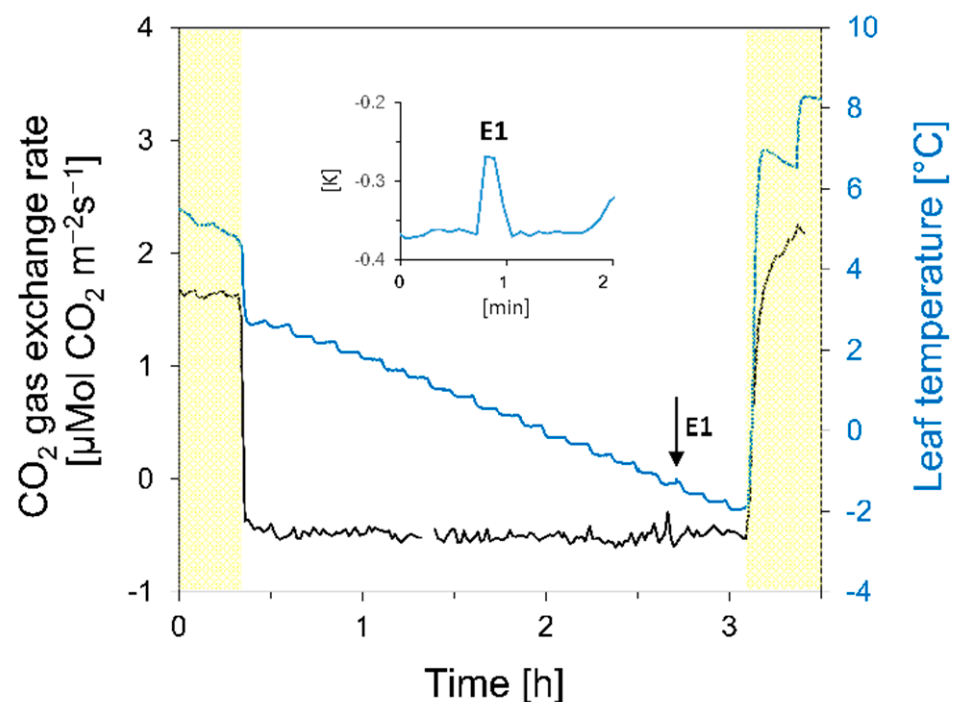

Figure 4. CO_2 gas exchange of *Solanum tuberosum* leaves recorded during controlled freezing treatments (−2 K·h^{-1}). Below +4 °C, the leaves were not irradiated (yellow shading: photosynthetic photon flux density 1000 μmol photons·m^{-2}·s^{-1}) and kept in darkness until thawing. At −1.2 °C, the first freezing event (E1) was registered, and after 24 min of being exposed to freezing temperatures, but without occurrence of the second freezing event (E2), the leaf was thawed. Black line: CO_2 gas exchange rate, blue lines: leaf temperature, arrow: freezing exotherm. The insert shows the freezing exotherm in the differential temperature plot (leaf−reference temperature).

3.2. Responses to the Second Freezing Event

3.2.1. Cytological Aspects

Leaf cross-sections of *S. tuberosum* were viewed with a light microscope during controlled freezing down to −2.9 °C (Figure 5). In the unfrozen state, the shape of the cells was unaffected when exposed to zero (Figure 5A) or the sub-zero temperature of −2.1 °C (Figure 5B). After ice formation, injuries were detected, especially in the spongy parenchyma cells (Figure 5C). Chloroplasts became invisible, likely due to fragmentation and destruction by intracellular ice formation. In lethally frozen cells, the entire cell lumen had a homogeneous, greenish, granular appearance. Cell walls of some spongy parenchyma cells were wrinkled. After thawing, at +5 °C, all spongy parenchyma cells appeared damaged, whereas in the palisade parenchyma, some cells seemed to have survived (Figure 5D). The damaged cells appeared flaccid, and cell sap leaked out.
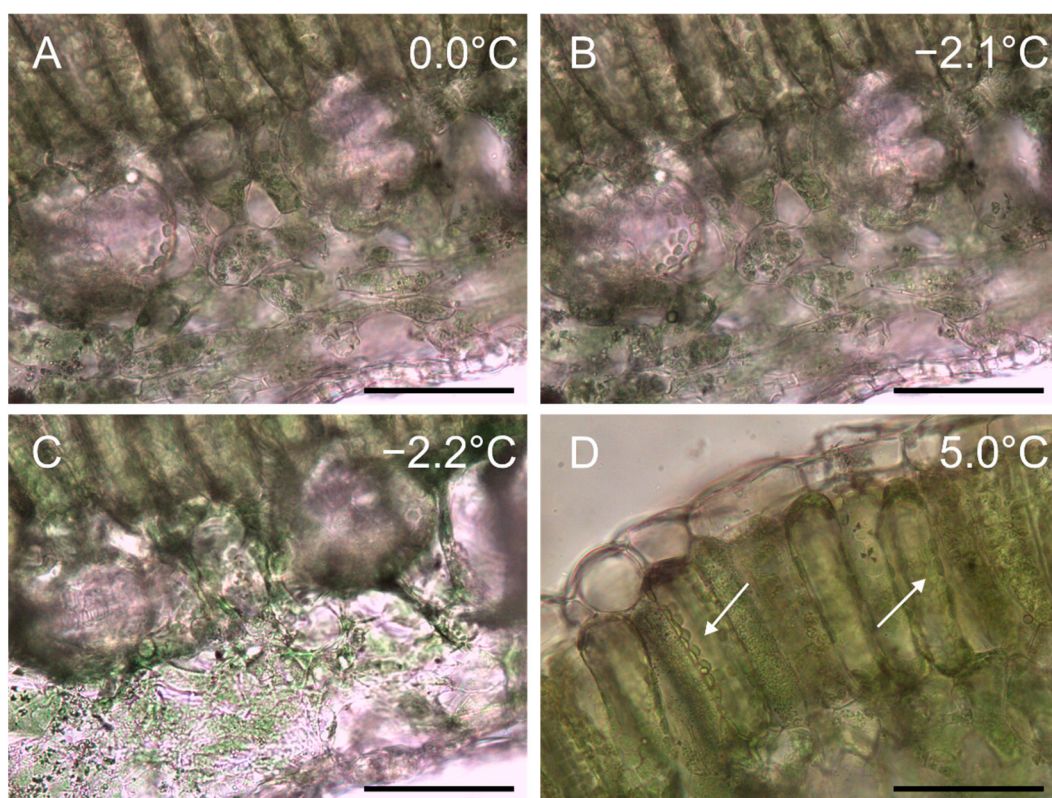
Figure 5. Images obtained from a cross-section of a leaf of *Solanum tuberosum* before and during a controlled freezing treatment down to −2.5 °C. Exposure to (**A**) zero and (**B**) a sub-zero temperature of −2.1 °C did not cause any visible changes. (**C**) Ice nucleation at −2.2 °C caused freezing injury to single cells. In the spongy parenchyma tissue, during freezing, the cells appeared destroyed. This was only partly the case in (**D**) the palisade parenchyma tissue, where single cells appeared undamaged (white arrows). Sample temperature is indicated at the top right corner. Black bars equal 100 μm.

3.2.2. Gas Exchange and Photosystem II

The dark respiration rate of the investigated potato leaf ranged between −0.3 and −0.5 μmol $CO_2 \cdot m^{-2} \cdot s^{-1}$ during controlled cooling in darkness and was unaffected by ice that formed at −1.0 °C during E1 (Figure 6). The second freezing process, E2, started at −2.5 °C, occurred 48 min after E1, and lasted approximately 35 min. Immediately after thawing, despite the onset of irradiation, no photosynthetic activity was measurable. An unchanged R_d was recorded. F_v/F_m, which was 0.79 before the freezing treatment, was 0.18, and the value successively decreased with the decay of cells. The day after, the leaf had lost its turgor and showed blackish discolorations, indicating necrosis.
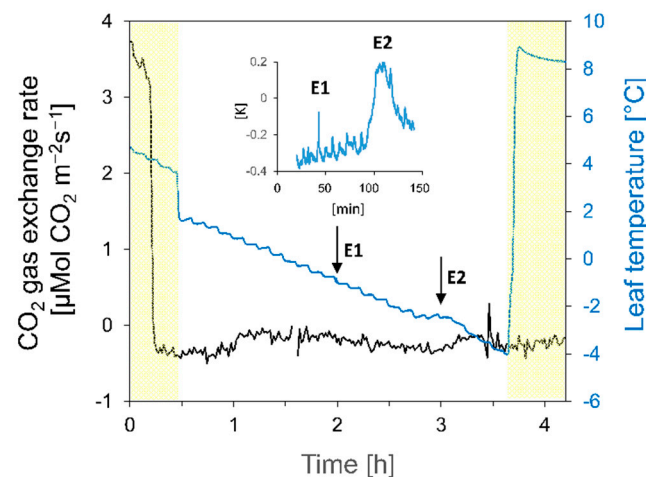
Figure 6. CO_2 gas exchange of a *Solanum tuberosum* leaf recorded during a controlled freezing treatment ($-2 \, \text{K} \cdot \text{h}^{-1}$). Below $+4 \, °\text{C}$, the leaves were not irradiated (yellow shading: photosynthetic photon flux density 1000 µmol photons$\cdot \text{m}^{-2} \cdot \text{s}^{-1}$) and kept in darkness until thawing. At $-1.0 \, °\text{C}$, the first freezing event (E1) was registered. A total of 48 min after E1, a distinct second freezing event (E2) was measured at $-2.5 \, °\text{C}$, which lasted for 35 min. Black line: CO_2 gas exchange rate, blue lines: leaf temperature, arrows: freezing exotherms. Insert shows the freezing exotherms in the differential temperature plot (leaf−reference temperature).

4. Discussion

4.1. Localization of Ice and Cellular Responses to the First Freezing Event

To test the consequences of the first freezing event, we measured gas exchange during non-destructive freezing and prepared semi-thin sections of freeze-fixed tissue frozen at a freezing rate, which would naturally occur. In frozen leaves, the dark respiration rate was unaffected, which indicates that gas exchange was not interrupted by ice. Non-injurious ice formation in intercellular spaces of the spongy tissue of evergreen leaves of *Hedera helix* and *Helleborus niger* was found to immediately block gas exchange, while in the ice-free mesophyll of *Pinus mugo*, even photosynthesis was possible [27]. Unaffected R_D in potato leaves upon E1 indicates that intercellular spaces are free of ice at this stage of the freezing process. Records of IDTA during E1 showed a rapid ice propagation along the vascular system, followed by a weak signal all over the leaf [9]. Our results show that this weak signal is not caused by ice formation in the intercellular spaces of the mesophyll but rather originates from thermal diffusion.

In leaves freeze-fixed after E1 and in frozen leaf cross-sections inspected with a light microscope, virtually all mesophyll cells appeared to be in a similar shape as seen in unfrozen samples. This means that upon E1, mesophyll cells of potato do not freeze-dehydrate. Usually, once extracellular ice has formed in a plant tissue, a steep water potential gradient between the extracellular ice masses and the supercooled liquid cell water forces freeze-dehydration, and the gradient increases with decreasing freezing temperature [20,28,29]. Mesophyll cells of many freezing-tolerant species have been shown to freeze-dehydrate in equilibrium (*Allium bulb scales* [30]; *Dendrosenecio keniodendron* [28]; *Hedera helix* [29]; *Sphagnum capillifolium* [31]; *Ranunculus glacialis* [32]) or non-ideal equilibrium (*Citrus* [33]; *Hordeum vulgare* [29]; *Pachysandra terminalis* [34]). In a recent study, it was found that freeze-dehydration is governed by cell wall thickness to cell size ratio and the relative area of intercellular spaces [35]. Furthermore, mesophyll cells of freezing-sensitive species can have extracellular ice and show cell collapse [36], which contrasts with our observation on potato mesophyll cells.

Similar to the findings here, mesophyll cells of several species have been shown to avoid freeze-dehydration and to keep the cell water inside the cell and to supercool (*Trachycarpus fortunei* [37]; *Sasa senanensis* [38]; *Pinus mugo* [27]) despite the presence of ice. However, potato mesophyll cells have a limited supercooling capacity. The supercooling

capacity of leaf tissues has been related to a specific leaf anatomy [20,35], and it has been shown to be fostered by narrow intercellular spaces and a densely package of mesophyll cells in usually sclerophyllous leaves [20]. *Solanum tuberosum* leaves are not sclerophyllous but have a small fraction of intercellular space (<1%) and would fulfill at least one anatomical trait that may aid supercooling. Intercellular spaces in herbaceous leaves with freeze-dehydrating mesophyll cells can be up to 35% [35]. Still, potato leaves have only a very low supercooling capacity. In a comparison of different *Solanum* species that differ in intercellular space size, no relationship to their freezing resistance was found [39]. Additionally, small-sized cells exhibited another important trait for supercooling, and this may be fulfilled in the mesophyll of *S. tuberosum*. The cell area of mesophyll cells of *S. tuberosum* is small. Compared to the freeze-dehydrating mesophyll cells of *R. glacialis* [32], spongy cells are a quarter the size, and palisade cells half the size.

Furthermore, it has been shown that stomatal density is increased in more ice-tolerant *Solanum* species [39], which somehow contradicts what others have found, i.e., that frost hardening of species of the same genus is coupled with decreased stomatal density (*Citrus* [40]; *Secale* sp. [41]).

4.2. The Second Freezing Event Is Intracellular

The second, thermally more pronounced freezing event occurs temporarily distinctly separated, up to 78 min later than E1, and coincides with frost damage. Freezing injuries to potato mesophyll cells are caused by intracellular ice formation that spontaneously occurs in supercooled cells. Until now, evidence for intracellular freezing was obtained by IDTA [9]. A second freezing exotherm, the so-called LTE, was indicative of intracellular freezing. The LTE was usually matched with frost damage. Our results show that after E2, mesophyll cells are damaged and unable to regain photosynthetic functions. This is clear, as in the cryo-light microscope, upon intracellular freezing, chloroplasts were seen to become invisible as chloroplasts were destroyed by ice formation. The methods employed in the current study additionally enabled visualizing the intracellular freezing processes during E2 at fully controlled freezing conditions. This is in contrast to several very early microscopic studies, where cooling of samples proceeded without control of freezing and thawing rates, cooling at unnaturally high freezing rates (2–4 K·min^{-1}), resulting in various degrees of artificial supercooling down to even -20 °C [15,20,42]. In these earlier studies [15,20,42], symptoms of intracellular freezing were that chloroplasts became invisible, likely due to fragmentation and destruction by intracellular ice growth. In lethally freeze-damaged cells, the entire cell lumen took on a homogeneous, greenish, granular appearance. Cell walls of some spongy parenchyma cells were wrinkled, cells appeared turgor-less, and cell sap seemed to leak out, which is a clear indication of membrane damage. Interestingly, in the palisade parenchyma, the damage pattern was unclear, as in some palisade parenchyma cells, the chloroplasts appeared unaffected. However, in most of the cells, the chloroplasts must have been ruptured as they virtually diminished and the chlorophyll occupied the entire cell volume. This corresponds to some extent to earlier microscopic observations upon intracellular freezing [15,20,42] that were mechanical destruction of biomembranes resulting from the fast growth of ice crystals, symptoms of frost plasmolysis (loss of osmotic responsiveness) after thawing, and complete destruction of cellular components visible in the light microscope, such as chloroplasts. Despite very simple measurement technologies, the symptoms found partly agree with our observations. Images of intracellularly frozen *Marchantia* protoplasts were shown by Sakai and Larcher [20], being recognizable as an instantaneous darkening of these cells, though precluding visibility of the ongoing processes. Already at low temperatures above the freezing point, aggregation of chloroplasts of *Marchantia polymorpha* indicates stress-induced cellular reorganization [43]. However, such a darkening symptom was never observed in our experiments during intracellular freezing of potato mesophyll cells. Asahina [15] also sometimes observed flash freezing (instantaneous darkening) on parenchymatous cells during rapid cooling (3–4 K·min^{-1}), but non-flash freezing could also occur. In non-flash freezing, several knife-like smooth ice

crystals grew parallel to another within a few seconds, and the cell contents were entirely concentrated between these ice crystals as a small number of irregular masses [15].

4.3. Outlook

Leaves of *S. tuberosum* are unable to frost-harden. We were able to show that after the first freezing event, the structural and physiological functionality of mesophyll cells fully remains. Still, upon the stochastic event of the second freezing, ice ruptures cellular membranes and brings immediate frost damage. Consequently, avoidance of ice formation is the only effective strategy to prevent potatoes from frost damage.

Supplementary Materials: The following material is available online at https://www.mdpi.com/article/10.3390/crops2040026/s1, Figure S1: Controlled freezing of *Solanum tuberosum* leaves. (A) The petioles of detached leaves were placed in cotton-filled Eppendorf tubes. Then, an aqueous suspension containing a small amount of ice nucleation active bacteria was added. The Eppendorf tubes were connected to each other using glass-fiber-coated wire that had previously been soaked in the same suspension. To prevent the fiberglass coating from drying out, the wire was inserted into a narrow polyvinyl chloride tube. The leaves were fixed on a polystyrene block. Fine-wire thermocouple sensors were positioned on the lower surface of the leaves to record the leaf temperature and, thus, also the ice formation in the leaf tissue. Wrapping the leaves in cling film increased the thermal insulation of the leaves during the freezing treatment. (B) The same leaves 1 h after thawing. For freeze-fixation, leaf discs (arrows) were punched out from the frozen leaves for subsequent high-pressure freeze-fixation. The leaves were completely undamaged by the freezing treatment applied (−2.5 °C for 20 to 35 min). (C) Leaf temperatures of the three leaves recorded during the freezing treatment. By connecting the Eppendorf tubes via the glass-fiber-coated wire, once nucleated, the ice was able to spread from the first frozen leaf to the others within 2 min (arrows indicate the freezing exotherms), so that all leaves froze almost simultaneously.

References

1. Reddy, B.J.; Mandal, R.; Chakroborty, M.; Hijam, L.; Dutta, P. A review on potato (*Solanum tuberosum* L.) and its genetic diversity. *Genetics* **2018**, *10*, 360–364. [CrossRef]
2. Glendinning, D.R. Potato introductions and breeding up to the early 20th century. *New Phytol.* **1983**, *94*, 479–505. [CrossRef]
3. Gu, L.; Hanson, P.J.; Mac Post, W.; Kaiser, D.P.; Yang, B.; Nemani, R.; Pallardy, S.G.; Meyers, T. The 2007 eastern US spring freezes: Increased cold damage in a warming world? *Bioscience* **2008**, *58*, 253–262. [CrossRef]
4. Richardson, D.G.; Weiser, C.J. Foliage frost resistance in tuber-bearing Solanums. *HortScience* **1972**, *7*, 19–22. [CrossRef]
5. Li, H.; Luo, W.; Ji, R.; Xu, Y.; Xu, G.; Qiu, S.; Tang, H. A comparative proteomic study of cold responses in potato leaves. *Heliyon* **2021**, *7*, e06002. [CrossRef]

6. Arora, R. Mechanism of freeze-thaw injury and recovery: A cool retrospective and warming up to new ideas. *Plant Sci.* **2018**, *270*, 301–313. [CrossRef]

7. Palta, J.P.; Weiss, L.S.; Harbage, J.F.; Bamberg, J.B.; Stone, J.M. Molecular mechanisms of freeze-thaw injury and cold acclimation in herbaceous plants: Merging physiological and genetic approaches. In *Interacting Stresses on Plants in a Changing Climate*; NATO ASI Series; Jackson, M.B., Black, C.R., Eds.; Springer: Berlin/Heidelberg, Germany, 1993; Volume 16, pp. 659–680.

8. Chen, P.M.; Burke, M.J.; Li, P.H. Frost hardiness of several solanum species in relation to freezing of water, melting-point depression, and tissue water content. *Bot. Gaz.* **1976**, *137*, 313–317. [CrossRef]

9. Stegner, M.; Schäfernolte, T.; Neuner, G. New insights in potato leaf freezing by infrared thermography. *Appl. Sci.* **2019**, *9*, 819. [CrossRef]

10. Li, P.H.; Huner, N.P.A.; Toivio-Kinnucan, M.; Chen, H.H.; Palta, J.P. Potato freezing-injury and survival, and their relationships to other stress. *AJPR* **1981**, *58*, 15–29. [CrossRef]

11. Chen, H.-H.; Li, P.H. Characteristics of cold acclimation and deacclimation in tuber-bearing *Solanum* species. *Plant Physiol.* **1980**, *65*, 1146–1148. [CrossRef]

12. Steffen, K.L.; Arora, R.; Palta, J.P. Relative sensitivity of photosynthesis and respiration to freeze-thaw stress in herbaceous species: Importance of realistic freeze-thaw protocols. *Plant Physiol.* **1989**, *89*, 1372–1379. [CrossRef]

13. Larcher, W. Physiological plant ecology. In *Ecophysiology and Stress Physiology of Functional Groups*; Springer: Berlin/Heidelberg, Germany, 2003.

14. Levitt, J. Responses of plants to environmental stresses. In *Chilling, Freezing, and High Temperature Stresses*; Academic Press: London, UK; New York, NY, USA, 1980.

15. Asahina, E. The freezing process of plant cells. *Contrib. Inst. Low Temp. Sci.* **1956**, *10*, 83–126.

16. Neuner, G.; Hacker, J. Ice formation and propagation in alpine plants. In *Plants in Alpine Regions: Cell Physiology of Adaptation and Survival Strategies*; Lütz, C., Ed.; Springer: Wien, Austria; New York, NY, USA, 2012; pp. 163–174.

17. Buchner, O.; Karadar, M.; Bauer, I.; Neuner, G. A novel system for in situ determination of heat tolerance of plants: First results on alpine dwarf shrubs. *Plant Methods* **2013**, *9*, 7. [CrossRef]

18. Buchner, O.; Steiner, P.; Andosch, A.; Holzinger, A.; Stegner, M.; Neuner, G.; Lütz-Meindl, U. A new technical approach for preparing frozen biological samples for electron microscopy. *Plant Methods* **2020**, *16*, 48. [CrossRef]

19. Burke, M.J.; Gusta, L.V.; Quamme, H.A.; Weiser, C.J.; Li, P.H. Freezing and injury in plants. *Annu. Rev. Plant Physiol.* **1976**, *27*, 507–528. [CrossRef]

20. Sakai, A.; Larcher, W. Frost survival of plants. In *Responses and Adaptation to Freezing Stress*; Springer: Berlin/Heidelberg, Germany; New York, NY, USA; London, UK; Paris, France; Tokyo, Japan, 1987; Volume 62, p. 321.

21. Ashworth, E.N.; Anderson, J.A.; Davis, G.A.; Lightner, G.W. Ice formation in Prunus persica under field conditions. *J. Amer. Soc. Hortic. Sci.* **1985**, *110*, 322–324. [CrossRef]

22. Neuner, G.; Bannister, P.; Larcher, W. Ice formation and foliar frost resistance in attached and excised shoots from seedlings and adult trees of *Nothofagus menziesii*. *N. Z. J. Bot.* **1997**, *35*, 221–227. [CrossRef]

23. Kuprian, E.; Munkler, C.; Resnyak, A.; Zimmermann, S.; Tuong, T.D.; Gierlinger, N.; Muller, T.; Livingston, D.P.; Neuner, G. Complex bud architecture and cell-specific chemical patterns enable supercooling of *Picea abies* bud primordia. *Plant Cell Environ.* **2017**, *40*, 3101–3112. [CrossRef]

24. Meindl, U.; Lancelle, S.; Hepler, P.K. Vesicle production and fusion during lobe formation in *Micrasterias* visualized by high-pressure freeze fixation. *Protoplasma* **1992**, *170*, 104–114. [CrossRef]

25. Holzinger, A.; Roleda, M.Y.; Lütz, C. The vegetative arctic freshwater green alga *Zygnema* is insensitive to experimental UV exposure. *Micron* **2009**, *40*, 831–838. [CrossRef]

26. Kuprian, E.; Tuong, T.D.; Pfaller, K.; Wagner, J.; Livingston, D.P.; Neuner, G. Persistent supercooling of reproductive shoots is enabled by structural ice barriers being active despite an intact xylem connection. *PLoS ONE* **2016**, *11*. [CrossRef]

27. Stegner, M.; Buchner, O.; Geßlbauer, M.; Lindner, J.; Floerl, A.; Xiao, N.; Holzinger, A.; Gierlinger, N.; Neuner, G. Frozen mountain pine needles: Endodermal confinement of ice and prevented freeze-dehydration of lignified mesophyll cells allow gas exchange. 2022; *submitted manuscript*.

28. Beck, E.; Schulze, E.-D.; Senser, M.; Scheibe, R. Equilibrium freezing of leaf water and extracellular ice formation in Afroalpine 'giant rosette' plants. *Planta* **1984**, *162*, 276–282. [CrossRef]

29. Hansen, J.; Beck, E. Evidence for ideal and non-ideal equilibrium freezing of leaf water in frosthardy Ivy (*Hedera helix*) and Winter Barley (*Hordeum vulgare*). *Bot. Acta* **1988**, *101*, 76–82. [CrossRef]

30. Palta, J.P.; Levitt, J.; Stadelmann, E.J. Freezing injury in onion bulb cells: I. Evaluation of the conductivity method and analysis of ion and sugar efflux from injured cells. *Plant Physiol.* **1977**, *60*, 393–397. [CrossRef]

31. Buchner, O.; Neuner, G. Freezing cytorrhysis and critical temperature thresholds for photosystem II in the peat moss *Sphagnum capillifolium*. *Protoplasma* **2010**, *243*, 63–71. [CrossRef]

32. Stegner, M.; Lackner, B.; Schäfernolte, T.; Buchner, O.; Xiao, N.; Gierlinger, N.; Holzinger, A.; Neuner, G. Winter nights during summer time: Stress physiological response to ice and the facilitation of freezing cytorrhysis by elastic cell wall components in leaves of a nival species. *Int. J. Mol. Sci.* **2020**, *21*, 7042. [CrossRef]

33. Anderson, J.; Gusta, L.; Buchanan, D.; Burke, M. Freezing of water in *Citrus* leaves. *J. Amer. Soc. Hortic. Sci.* **1983**, *108*, 397–400. [CrossRef]

34. Zhu, J.-J.; Beck, E. Water relations of *Pachysandra* leaves during freezing and thawing: Evidence for a negative pressure potential alleviating freeze-dehydration stress. *Plant Physiol.* **1991**, *97*, 1146–1153. [CrossRef]

35. Stegner, M.; Floerl, A.; Lindner, J.; Plangger, S.; Schäfernolte, T.; Strasser, A.; Thoma, V.; Walde, J.; Neuner, G. Freeze dehydration vs. supercooling of mesophyll cells: Impact of cell wall, cellular and tissue traits on the extent of water displacement. *Physiol. Plant.* 2022; *accepted manuscript*. [CrossRef]

36. Ashworth, E.N.; Pearce, R.S. Extracellular freezing in leaves of freezing-sensitive species. *Planta* **2002**, *214*, 798–805. [CrossRef]

37. Larcher, W.; Meindl, U.; Ralser, E.; Ishikawa, M. Persistent supercooling and silica deposition in cell walls of palm leaves. *J. Plant Physiol.* **1991**, *139*, 146–154. [CrossRef]

38. Ishikawa, M.; Oda, A.; Fukami, R.; Kuriyama, A. Factors contributing to deep supercooling capability and cold survival in dwarf bamboo (*Sasa senanensis*) leaf blades. *Front. Plant Sci.* **2014**, *5*, 791. [CrossRef]

39. Palta, J.P.; Li, P.H. Frost-hardiness in relation to leaf anatomy and natural distribution of several *Solanum* species. *Crop Sci.* **1979**, *19*, 665–671. [CrossRef]

40. Hirano, E. Relative abundance of stomata in Citrus and some related genera. *Bot. Gaz.* **1931**, *92*, 296–310. [CrossRef]

41. Huner, N.P.A.; Palta, J.P.; Li, P.H.; Carter, J.V. Anatomical changes in leaves of puma rye in response to growth at cold-hardening temperatures. *Bot. Gaz.* **1981**, *142*, 55–62. [CrossRef]

42. Cox, W.; Levitt, J. An improved, leaf-disk method for determining the freeze-killing temperature of leaves. *Cryobiology* **1972**, *9*, 251–256. [CrossRef]

43. Tanaka, H.; Sato, M.; Ogasawara, Y.; Hamashima, N.; Buchner, O.; Holzinger, A.; Toyooka, K.; Kodama, Y. Chloroplast aggregation during the cold-positioning response in the liverwort *Marchantia polymorpha*. *J. Plant Res.* **2017**, *130*, 1061–1070. [CrossRef]